

# Elastoplastic nonlinear behavior of planar steel gabled frame

Sina Heyrani Moghaddam\* and Amir R. Masoodi<sup>a</sup>

*Department of Civil Engineering, Ferdowsi University of Mashhad, Iran*

*(Received March 8, 2019, Revised June 6, 2019, Accepted July 2, 2019)*

**Abstract.** In this paper, static nonlinear analysis of gable frame is performed using OpenSees software. Both geometric and material nonlinearities are considered in analyses. To consider large displacements, co-rotational coordinate transformation is used in software. The effects of symmetric and asymmetric support conditions including clamped and simple supports are studied. On the other hand, the material nonlinearity is reflected on analyses using Giuffre-Menegotto-Pinto steel material. Note that strain hardening characteristics are also considered in this model. Moreover, I-shaped cross-section is assumed for all members. The results are provided for different geometry properties of gable frame including shallow and deep inclined roof. It should be added that buckling and post-buckling behaviors of gable frame are investigated using related equilibrium paths. A comparison study is also implemented on the responses of buckling loads obtained for different support and geometry conditions. To trace snap-through paths completely, a displacement control method entitled arc-length is utilized. Findings show the capability of proposed model in nonlinear analysis of gable frames.

**Keywords:** nonlinear analysis; co-rotational; strain hardening; buckling and post-buckling; steel gable frame; OpenSees software

---

## 1. Introduction

Gable frames are extensively used as industrial structures which have wide bays without middle columns. These structures are constructed with steel materials which have nonlinear behavior. On the other hand, these structures should have capability to undergo different types of loads including dead, live, snow and wind loads. It is obvious that these structures have low weight. Therefore, nonlinear behavior of structure plays an essential role in parameters of optimum design. It should be added that most of these structures are constructed with I-shape section due to high moment of inertia. These parts are subjected to axial, shear forces and bending moments, simultaneously. To obtain the exact behavior of structure, using nonlinear analysis is necessary. It should be added that nonlinear behaviors include geometric and material. Geometric nonlinear analysis can incorporate the effects of large displacements while the material nonlinear analysis considers the effects of nonlinear stress-strain behavior of material on the displacements and stresses of structures. In general, both geometric and material nonlinearities should be considered

---

\*Corresponding author, M.Sc., E-mail: [sina.heyрани@mail.um.ac.ir](mailto:sina.heyрани@mail.um.ac.ir)

<sup>a</sup> Ph.D. Candidate

in the nonlinear analysis to predict the exact behavior of structures with various support conditions.

Using an efficient model for steel material is one of the significant part of this research. A uniaxial material model was originally proposed by Menegotto and Pinto. It could simulate the cyclic response of steel (Menegotto and Pinto 1973). Moreover, it was widely utilized to simulate the dynamic response of steel members discretized by means of fibres (Salawdeh and Goggins 2013, Atlayan and Charney 2014). Due to simplicity of this formulation, it was employed in many programs to obtain of the response of structures such as OpenSees (McKenna *et al.* 2006). The first formulation of this model, which has been published by (Giuffrè 1970), drew their origin from a previous research study by Goldberg and Richard (Goldberg and Richard 1963). This model was developed by Menegotto and Pinto to simulate kinematic hardening (Menegotto and Pinto 1973). In the early 1980s, Filippou *et al.* improved the Menegotto and Pinto model to consider isotropic hardening (Filippou *et al.* 1983).

Several researches were performed about buckling analysis of 2D frame. Some of them investigated the buckling load of frame using analytical solution (Masoodi 2018, Rezaiee-Pajand and Masoodi 2018). In these researches, a beam or beam-column element was formulated to use in elastic or inelastic buckling analyses. In other researches, numerical methods were employed to present the buckling behavior of frames. Furthermore, post-buckling behavior of frames can be also investigated in this way (Ottaviani 1975, Care *et al.* 1977, Wood and Zienkiewicz 1977, El-Zanaty and Murray 1983, Kassimali and Garcilazo 2010, Dere and Dede 2011, Taeprasartsit 2013, Thombare *et al.* 2016, Rezaiee-Pajand *et al.* 2019, Rezaiee-Pajand *et al.* 2019). The advantage of these studies was the ability of method to predict the post-buckling behavior of structures using the obtained equilibrium paths.

Recently, some new researches were also developed about nonlinear analysis of gable frame. In an old research, large deformation analysis of portal frame was studied by (Oran and Kassimali 1976). In addition, large deformation elastic-plastic analysis of space frames was presented by (Abbasnia and Kassimali 1995). Recently, free vibration and dynamic analysis of gable frame was implemented using OpenSees software by (Shooshtari *et al.* 2014, Masoodi and Heyrani-Moghaddam 2015). In 2016, the static nonlinear analysis of gable frame was also performed by (Shooshtari *et al.* 2015). Furthermore, another research was performed on the nonlinear dynamic analysis of slender portal frame under base excitation by Paullo Muoz *et al.* They obtained the responses in frequency domain (Paullo Muoz *et al.* 2017).

One of effective assumptions in static analysis of 2D frames is the consideration of types of connections including fixed or simple. In the past, so many researches have been done about semi-rigid frame analysis. Linear and non-linear free vibration analysis of frames having semi-rigid connections using a numerical solution was implemented by (Chan and Ho 1994). They used rotational springs for modeling the nodal connections and introduced direct stiffness matrix. Further, the effects of non-linear semi-rigid connections on static and dynamic analysis of spatial frames were investigated by (Shi and Atluri 1989). Some other researches were also developed in those years about investigating the linear and nonlinear behavior of steel frames constructed with linear or nonlinear connections (Fu *et al.* 1998, Rodrigues *et al.* 1998, Rezaiee-Pajand *et al.* 2018, Rezaiee-Pajand *et al.* 2018, Rezaiee-Pajand *et al.* 2018, Rezaiee Pajand *et al.* 2018, Rezaiee-Pajand and Masoodi 2019).

The aim of this research is nonlinear analysis of gable frame with different geometry and support conditions. It is worth mentioning that both geometric and material nonlinearities are incorporated in the analyses. To consider large deformation, co-rotational formulation is employed.

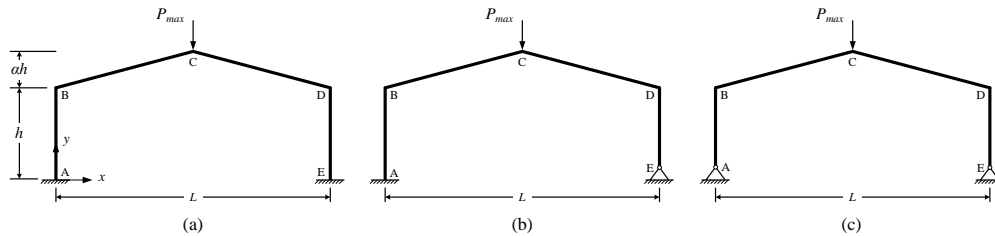


Fig. 1 The geometry of gable frames

Table 1 Height of inclined part of gable frames

$\alpha$	$h' = \alpha h$ (m)
0.2	1.0
0.4	2.0
0.6	3.0
0.8	4.0

It should be added that arc-length nonlinear solution method is also utilized to trace the relevant equilibrium paths completely, especially snap-trough ones. In addition, the Giuffre-Menegotto-Pinto steel material properties along with strain hardening are used for material nonlinearity. Moreover, different cases are considered for the geometry of inclined part of gable frame so that the slope of roof is equal to 20, 40, 60 and 80 percent. The results are reported as equilibrium paths to show the buckling and post-buckling behavior of gable frames. In each part, the buckling load is also reported separately. Outcomes show the accuracy and capability of OpenSees software in nonlinear analysis of frames.

## 2. Geometry of structure

The geometry of gable frame is depicted in Fig. 1. In the illustration,  $h$  defines the height of columns. Moreover, the length of bay is specified by  $L$ . It should be added that the geometry of frame is symmetric. Three states are considered for the support conditions including clamped-clamped, clamped-simple and simple-simple. These states are shown in Fig. 1(a,b,c).

It is assumed that the connection of all members is rigid. So the flexibility of connections and supports is ignored. To enhance the accuracy of responses, each member is discretized by five nonlinear beam-column elements in OpenSees software (OpenSees 2006). Therefore, 21 nodes are defined in this model. On the other hand, numerical integration is performed using 7-Gauss points. In this research, the length and height of gable frame are equal to 15 and 5 meter, respectively. In addition, the height of inclined part of frame is defined as a coefficient of frame height ( $h$ ). The parameter  $\alpha$  is assigned to this ratio. This parameter changes from 0.2 to 0.8. Table 1 report the height of inclined part of gable frame according to values of  $\alpha$ .

The type of loading in this study is static. So a point load is applied at the top point of the frame (Point C). The load is applied incrementally from zero up to maximum value of 1080 KN. This value is considered to achieve the complete equilibrium path of the frame including snap-through and snap-back parts. The analysis is performed using displacement control method.

### 3. FE modeling

The relation between stress and strain considering isotropic elastic material can be expressed as follow

$$\boldsymbol{\sigma}_i = \mathbf{C}_i \boldsymbol{\varepsilon}_i \quad (1)$$

where  $C_i$  is the elastic material matrix. The strain vector can be given below

$$\boldsymbol{\varepsilon}_i = \mathbf{D}_f \mathbf{N}_i \mathbf{d}_i \quad (2)$$

in which  $D_f$  is the differential operator matrix. The element local displacement vector is defined by  $d_i$ . It is worth mentioning that the relation between element local and global displacement vectors can be presented as follow

$$\mathbf{D}_i = \mathbf{D}_i^r + \mathbf{T}_i \mathbf{d}_i \quad (3)$$

in which  $D_i$  is the element nodal displacement vector in global coordinates and  $D_i^r$  is the rigid body displacement vector in global coordinates. It is noted that  $T_i$  is the transformation matrix which can be defined as follow

$$\mathbf{T}_i = \begin{bmatrix} \cos \alpha & -\sin \alpha & 0 & 0 & 0 & 0 \\ \sin \alpha & \cos \alpha & 0 & 0 & 0 & 0 \\ 0 & 0 & 1 & 0 & 0 & 0 \\ 0 & 0 & 0 & \cos \alpha & -\sin \alpha & 0 \\ 0 & 0 & 0 & \sin \alpha & \cos \alpha & 0 \\ 0 & 0 & 0 & 0 & 0 & 1 \end{bmatrix} \quad (4)$$

The strain energy of the element  $\Pi_i$  is

$$\Pi_i = \frac{1}{2} \int_{V_i} \boldsymbol{\sigma}_i^T \boldsymbol{\varepsilon}_i dV_i \quad (5)$$

By substituting the Eq. (2) into Eq. (5) and simplifying, the following relation can be found

$$\Pi_i = \frac{1}{2} \mathbf{d}_i^T \mathbf{k}_i \mathbf{d}_i \quad (6)$$

where  $k_i$  is the symmetric elemental stiffness matrix that can be calculated by using the below equation

$$\mathbf{k}_i = \int_{V_i} \mathbf{B}_i^T \mathbf{C}_i \mathbf{B}_i dV_i \quad (7)$$

It should be added that  $B_i$  is the strain matrix that is equal to  $D_f N_i$ . This matrix includes axial and bending stiffness matrix  $k_1$  and geometric stiffness matrix  $k_2$ , as given

$$\mathbf{k}_i = \mathbf{k}_1 + \mathbf{k}_2 \quad (8)$$

It is worth mentioning that the strain energy can be rewritten by substituting Eq. (3) into Eq. (6)

$$\Pi_i = \frac{1}{2} \left( \left( \mathbf{T}_i^T (\mathbf{D}_i - \mathbf{D}_i^r) \right)^T \mathbf{k}_i \mathbf{T}_i^T (\mathbf{D}_i - \mathbf{D}_i^r) \right) = \frac{1}{2} \mathbf{D}_i^{\text{tr}} \mathbf{K}_i \mathbf{D}_i \quad (9)$$

where  $\mathbf{K}_i$  is the stiffness matrix of the element in fixed global coordinate system. It is calculated as follow

$$\mathbf{K}_i = \mathbf{T}_i \mathbf{k}_i \mathbf{T}_i^T \quad (10)$$

By using the global stiffness matrix and using arc-length iterative solution method, the nonlinear analysis of the structure can be carried out.

#### 4. Nonlinear analysis principles

To consider large deformation of structure, a nonlinear beam-column element which is defined in OpenSees software is employed based on the corotational principles. This method divides the deformation of element into two separate parts including rigid body motion and elastic displacements. Therefore, the stiffness matrix of element is constructed by elastic and tangent stiffness matrices. It is worth mentioning that some researches were implemented about developing corotational formulations of beam-column element (Hsiao *et al.* 1999, Urthaler and Reddy 2005, Chen *et al.* 2006, Liang *et al.* 2016). For the corotational element, the following relation can be used to achieve the vector of the internal force and tangent stiffness matrix.

$$p = \frac{\partial U}{\partial \mathbf{u}} \quad , \quad \mathbf{K} = \frac{\partial p}{\partial \mathbf{u}} = \mathbf{K}_M + \mathbf{K}_G \quad (11)$$

in which  $\mathbf{K}_M$  is Material Stiffness Matrix and  $\mathbf{K}_G$  is Geometric Stiffness Matrix. Moreover,  $p$  is the internal force vector which is obtained by differentiating the total strain energy with respect to displacement vector of  $u$ . To solve the nonlinear equations, displacement control method is utilized. It is worth mentioning that load control method cannot be used in this analysis. Based on the obtained equilibrium paths, it is necessary to use a displacement control method to trace the snap-trough paths completely. Several strategies were also developed by other researches to solve nonlinear equations (Batoz and Dhatt 1979, Powell and Simons 1981). These researches were performed to resolve the problem of limit points which cannot be passed by load control methods. In some other methods, the iterative procedure is controlled using displacement or combination of displacement and load (Haisler *et al.* 1977, Clarke and Hancock 1990). Moreover, another solution method in which a constraint is used to limit the load increment. This method was also developed by (Crisfield 1983, Fafard and Massicotte 1993, Rose *et al.* 2016). In this study, a displacement control method which has been developed in OpenSees software is employed to obtain the related equilibrium paths having snap-trough. In this method, the governing finite element equation is obtained at  $t+\Delta t$  as follow

$$R(U_{t+\Delta t}, \lambda_{t+\Delta t}) = \lambda_{t+\Delta t} F^{ext} - F(U_{t+\Delta t}) \quad (12)$$

in which  $F(U_{t+\Delta t})$  is the vector of internal forces. It is worth mentioning that these are obtained based on the displacement  $U_{t+\Delta t}$ . Moreover, the external load is defined by  $F^{ext}$  and  $\lambda$  is the load factor which is updated at each step. The linearized form of the Eq. (12) is given by

$$K_{t+\Delta t}^{*i} \Delta U_{t+\Delta t}^{i+1} = (\lambda_{t+\Delta t}^i + \Delta \lambda^i) F^{ext} - F(U_{t+\Delta t}) \quad (13)$$

In fact, this equation includes  $n$  equations and  $n+1$  unknown parameters. As a result, to solve the system of equations, an extra equation is also required. In this procedure, the first external load factor used for the first step should be specified by the analyzer at the identified point at which the external load applied.

## 5. OpenSees Modelling

In this section, the properties of materials which have been employed in this analysis are defined. The details of material behavior are also presented here. It should be added that the nonlinear behavior of materials is considered in this analysis. Moreover, two different types of analysis including geometric and material nonlinear are considered. It is worth mentioning that the gable frame is modeled as a two-dimensional frame. The number of degrees of freedom is equal to three including two translational and one rotational. The following information is employed for this model.

### 5.1 Geometric nonlinear analysis

Based on the co-rotational nonlinear formulation, the large displacement and rotation of element can be implemented in the analysis. This method is defined as a “geomtransf” at the OpenSees software. The co-rotational formulation is based on small strain beam theory. It has two coordinate systems including the fixed global and the element co-rotational local coordinate systems. The rotation and translation of the co-rotational local frame are performed with each element but the deformation is not. This formulation separates the rigid body motion from the pure deformation. The deformation part is always small relative to the co-rotational element frame deformation. To fulfill this goal, a nonlinear beam-column element is employed for discretizing. It should be added that static analysis of frame structures is carried out in the current study.

### 5.2 Material

Two different types of material are employed in this analysis. First, an elastic material in which the elastic modulus is equal to  $2.1 \times 10^{11} \text{ N/m}^2$  is defined. Also, it is not necessary to determine the fracture point and so the structure is not failed due to material capacity loss. On the other hand, to consider the nonlinear behavior of material, nonlinear steel material entitled “Steel 02” is used. It is worth mentioning that the material is defined as a uniaxial material in OpenSees software. Note that isotropic strain hardening is also considered for the inelastic material. The elastic modulus and the yielding stress are equal to  $2.1 \times 10^{11} \text{ N/m}^2$  and  $2.4 \times 10^8 \text{ N/m}^2$ , respectively. The Poisson’s ratio is equal to 0.3 for both elastic and inelastic materials. Other characteristics of the material which are related to nonlinear behavior and strain hardening are also defined as follow

$$\begin{aligned} b &= 0.1 \\ R_0 &= 18 & R_1 &= 0.952 & R_2 &= 0.15 \\ a_1 &= 0 & a_2 &= 1 & a_3 &= 0 & a_4 &= 1 \end{aligned} \quad (14)$$

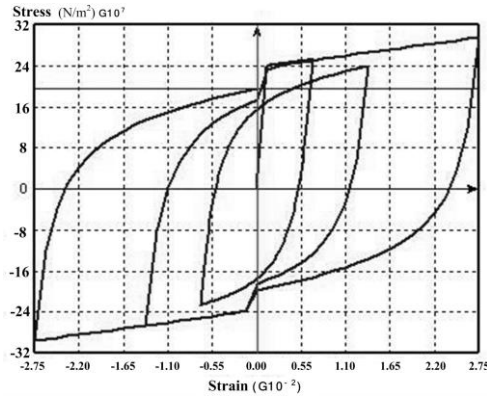


Fig. 2 Stress-strain curve of nonlinear steel material

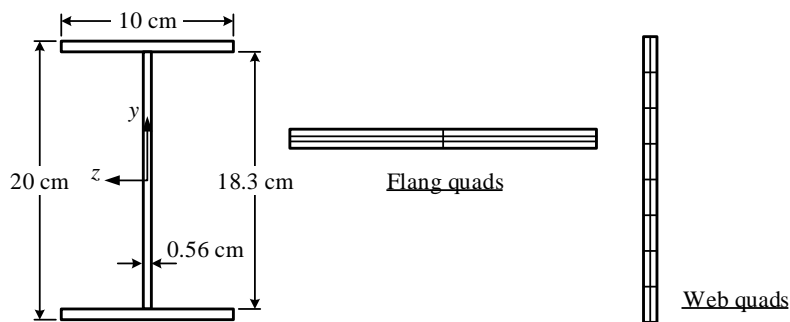


Fig. 3 The geometry properties of I-shape cross-section

in which  $b$  is the ratio of isotropic strain hardening. In other words, it is equal to the ratio of secondary elastic modulus to initial one. The parameter  $R_i$  ( $i= 0,1,2$ ) is used to control the transition between elastic to plastic region at the stress-strain curve. Moreover, the factors  $a_i$  ( $i= 1,2,3,4$ ) present the increase of compression and tension yielding pushes. It is worth mentioning that no isotropic hardening can be achieved by using the aforementioned factors. Further, the schematic of stress-strain curve of material having the above properties is depicted in Fig. 2

### 5.3 Cross-section

In this study, an I-shape cross-section is considered for the all members of gable frame including columns and beams. It should be added that this section is defined using fiber section in OpenSees. Also, the cross-section is divided into several quads (see Fig. 3). The geometry properties of cross-section are illustrated in Fig. 3. All dimensions are in *cm*.

### 5.4 Loading

The type of loading is static. So static bending analysis has been carried out in this article. The frame undergoes a point load at the point C (top of the frame). The type of loading in this research is static and its direction is along  $y$ -axis (See Fig. 1).

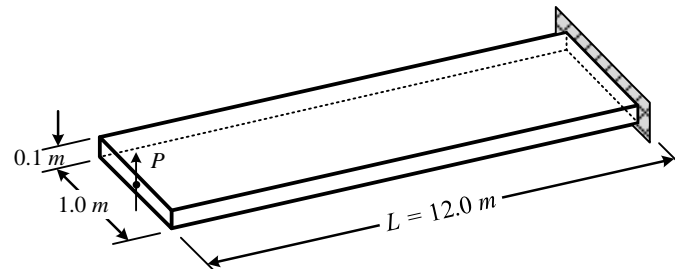


Fig. 4 A cantilever beam subjected to free end shear load

### 5.5 Element

The element used in this study is a nonlinear beam-column element which has been formulated based on a displacement-based beam element. This element has been defined in OpenSees software. The number of element used for discretizing each member is equal to five.

### 5.6 Nonlinear solution method

Based on the aforementioned in previous section, arc-length method is utilized to trace the equilibrium paths completely, especially snap-through ones (Crisfield 1983, Memon 2004, Rose *et al.* 2016).

## 6. Numerical study

In this section, a verification study is carried out to show the correctness and accuracy the model used in this article. In this verification, a convergence study is also performed to achieve the optimum number of elements required for discretization of members. Afterwards, the nonlinear behavior of gabled frames with different boundary conditions will be studied. To implement the numerical integration, seven gauss points are used along the length of element. To trace the fully nonlinear equilibrium paths of the structures, arc-length method is employed which can pass the limit points of load and displacement.

### 6.1 Cantilever beam under end shear load

A cantilever beam subjected to end shear force is investigated in this example. The free end point load is incrementally applied up to 4. The elastic modulus and Poisson's ratio of the material are equal to  $1.2 \times 10^6 \text{ N/m}^2$  and 0.3, respectively. The geometric properties of the structure are depicted in Fig. 4. In addition, Nanakorm and Vu solved this problem by using five beam and Rezaiee-Pajand *et al.* used 32 triangular shell elements for solving this problem (Jeon *et al.* 2015, Rezaiee-Pajand *et al.* 2018).

The equilibrium paths related to horizontal and vertical displacements of the free end are presented in Fig. 6. In this figure, N represents the number of element used for discretization. The results are provided for different number of elements including 1, 2, 5 and 10 elements to carry out a convergence study. Moreover, the responses are compared with the reference solutions (Jeon *et al.* 2015).

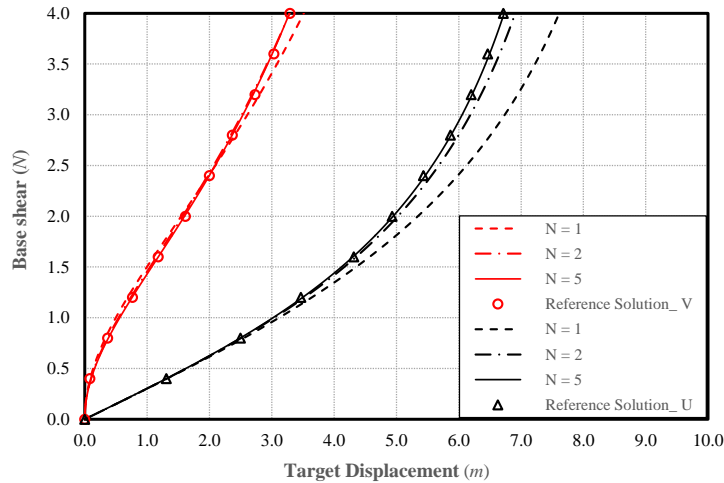


Fig. 5 The equilibrium paths of the cantilever beam subjected to end shear load

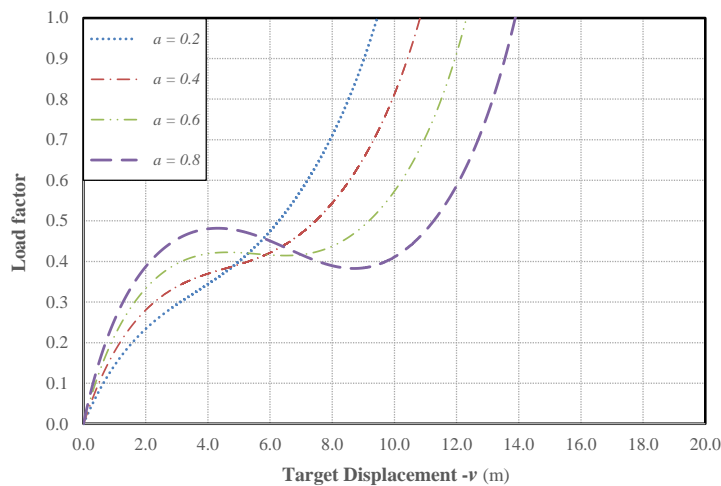


Fig. 6 The equilibrium path of gable frame having fixed supports considering geometric nonlinearity

### 6.2 Gable frame with fixed-fixed supports

In this part, the responses, which are obtained using OpenSees software, are presented for different states of gable frame. It is worth mentioning that equilibrium paths are provided for each case in which the support conditions and the angle of inclined part of frame change. On the other hand, the equilibrium paths are provided for two cases of analyses including geometric and both geometric and material nonlinearities. First, the results of geometric nonlinear analysis are reported. Then, the related results of geometric and material nonlinear analysis are presented. Accordingly, Fig. 6 shows the equilibrium path of the gable frame having fixed supports (See Fig. 1(a)). It should be added that geometric nonlinearity is considered in this analysis.

It is observed that type of buckling load occurring in this structure is limit state buckling.

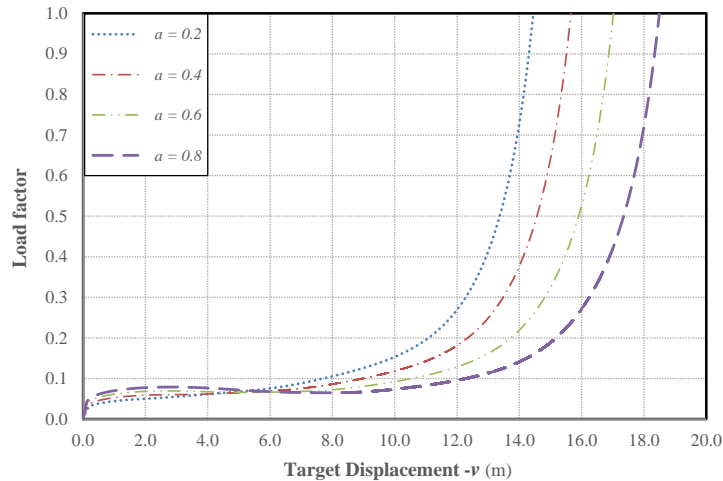


Fig. 7 The equilibrium path of gable frame having fixed supports considering geometric and material nonlinearities

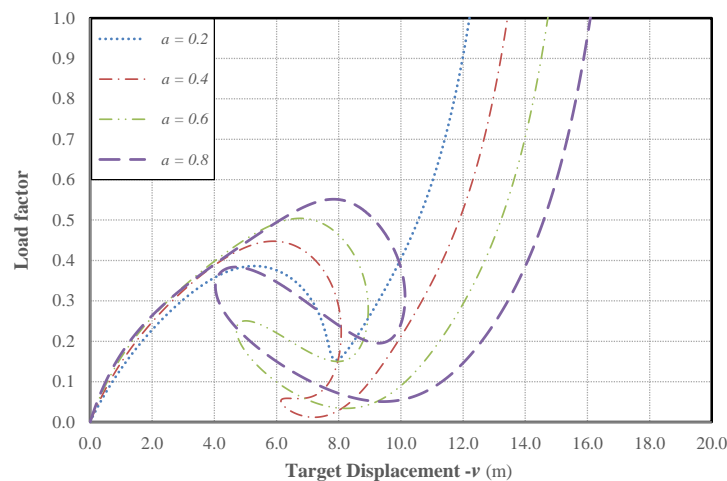


Fig. 8 The vertical displacements of gable frame having fixed and simple supports considering geometric nonlinearity

Therefore, a limit point is expected to be observed in the equilibrium path. Moreover, the first buckling load of the frame in which the slope of inclined part is greater than the others is more. Accordingly, the buckling load of the frame with  $a = 0.8$  is almost equal to  $0.4816P_{max}$  while this load decreases for the lower values of the ratio  $a$ . On the other hand, the first buckling load is not observed in the equilibrium paths of the gable frame with the ratio of almost  $a \leq 0.5$ . It should be added that the capacity of the gable frame in which the value of slope ratio is greater than the others is more than the other frames. Therefore, the maximum displacement of the target point at the end of loading shows the ductility of the frame. The related equilibrium path which is obtained based on the both geometric and material nonlinear analysis of fixed support gable frame is also provided in Fig. 7.

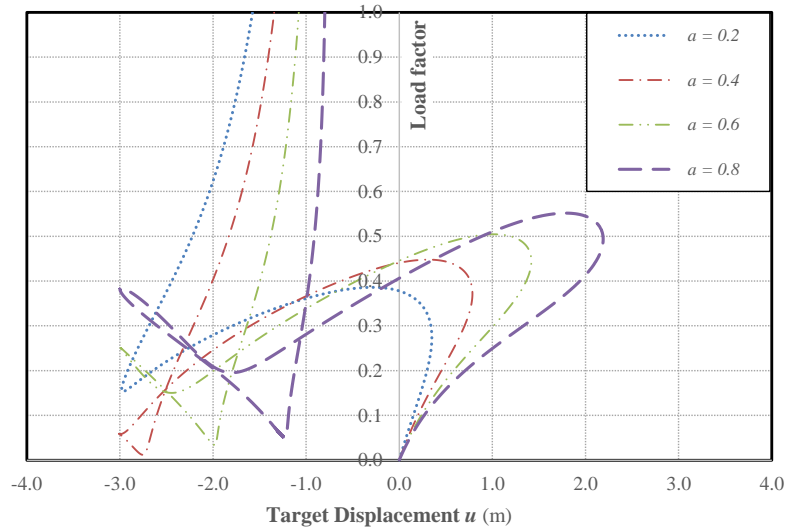


Fig. 9 The horizontal displacements of gable frame having fixed and simple supports considering geometric nonlinearity

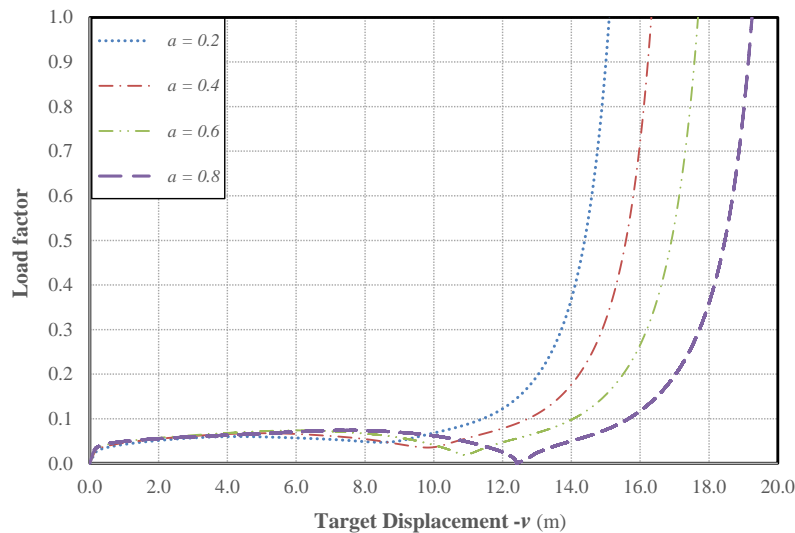


Fig. 10 The vertical displacements of gable frame having fixed and simple supports considering geometric and material nonlinearities

It is obvious that the buckling capacity of the gable frame decreases when the material nonlinearity is also added to the nonlinear analysis. These equilibrium paths also depicts the more ductility for the gable frame with the greater values of slope ratio  $a$ . The maximum value of vertical displacement increases when the both nonlinearities are considered. On the other hand, the buckling capacity of the gable frame in geometric and material nonlinear analysis reduces almost 84.5 percent in relative to the geometric nonlinear analysis responses.

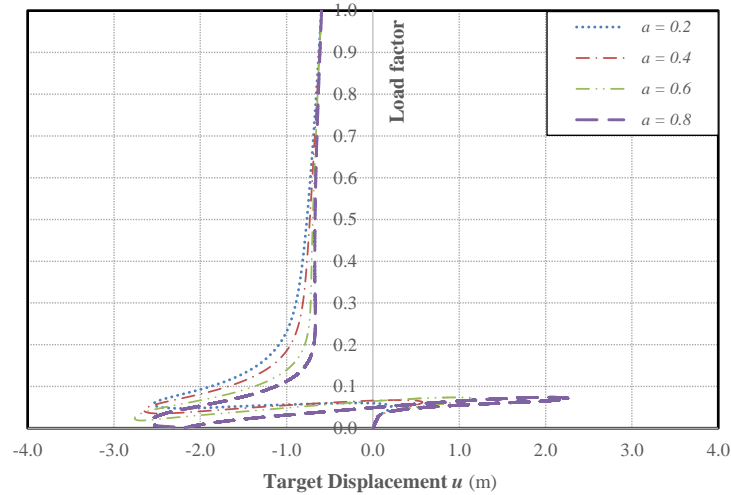


Fig. 11 The horizontal displacements of gable frame having fixed and simple supports considering geometric and material nonlinearity

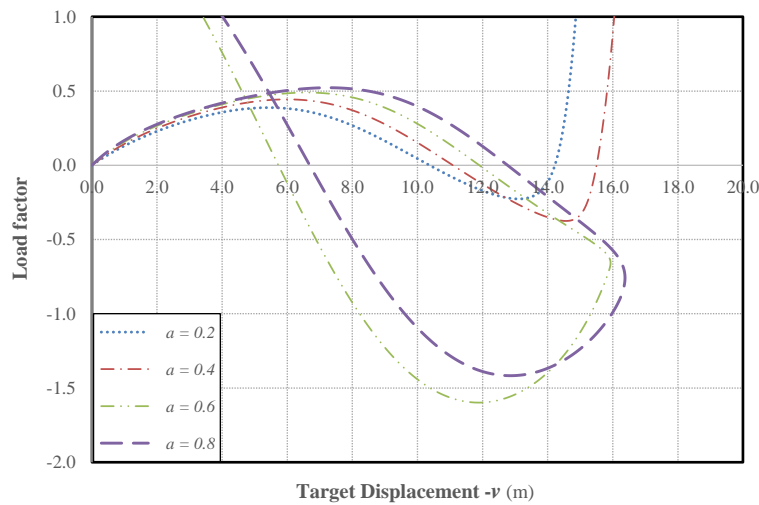


Fig. 12 The equilibrium path of the simply supported gable frame considering geometric nonlinearity

### 6.3 Gable frame with fixed-simple supports

To investigate the effects of support conditions on the buckling and post-buckling behavior of the gable frame, another state in which the asymmetric support condition including fixed and simple support for the columns is also considered (See Fig. 1(b)). Fig. 8 and Fig. 9 depict the related equilibrium paths of the gable frame with this support conditions. It is worth mentioning that geometric nonlinear analysis is performed to obtain these results. Fig. 8 is related to the vertical displacement. Moreover, due to asymmetry, the horizontal displacements of the point C are reported in Fig. 9.

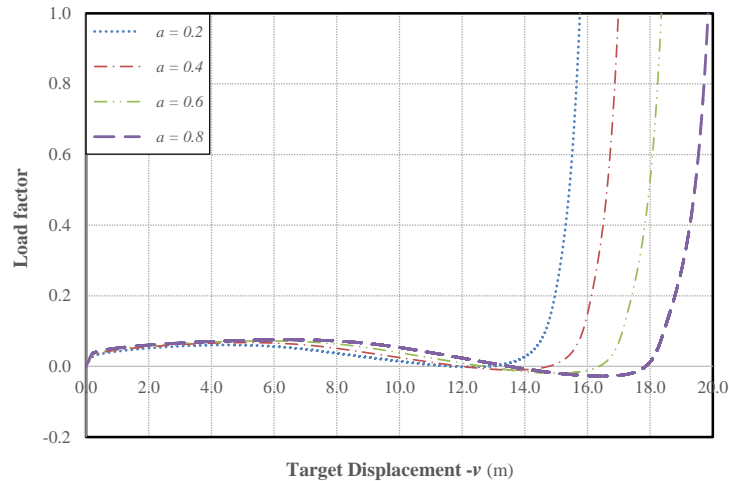


Fig. 13 The equilibrium path of the simply supported gable frame considering geometric and material nonlinearities

Table 1 The buckling load of gable frame with different support conditions and roof slope ratio

Support Condition	Slope ratio $a$	$P_{cr} (\times P_{max})$	
		Geometric nonlinear	Geometric and material nonlinear
C-C	0.2	-	-
	0.4	-	-
	0.6	0.4227	0.0695
	0.8	0.4816	0.0789
C-S	0.2	0.3859	0.0602
	0.4	0.4478	0.0676
	0.6	0.5044	0.0739
	0.8	0.5516	0.0743
S-S	0.2	0.3882	0.0606
	0.4	0.4443	0.0673
	0.6	0.4894	0.0721
	0.8	0.5219	0.0754

It is observed that the behavior of the asymmetric gable frame is more complicated than the symmetric frame. On the other hand, the nonlinear responses including vertical and horizontal displacements based on the geometric and material nonlinearities are also reported in Fig. 10 and Fig. 11, respectively.

#### 6.4 Gable frame with simple-simple supports

Finally, a simply supported gable frame which is shown in Fig. 1(c) is analyzed. The geometric nonlinear responses are reported in Fig. 12 while the results of geometric and material nonlinear

analysis are presented in Fig. 13.

It is obvious that increasing the slope ratio causes that the equilibrium path of the gable frame obtained in geometric nonlinear analysis tends to be more complicated. It is concluded that for the slope ratio with the approximate value of  $a \geq 0.5$ , there is no snap-back in the equilibrium paths of the frame in geometric nonlinear analysis while all of the equilibrium paths of the frame in both geometric and material nonlinear analysis is smooth and have a snap-trough behavior. On the other hand, the ductility of the gable frame with simple supports is more than that of gable frames having other support conditions.

The first buckling load of gable frame with various support conditions is presented in Table 2. In this table C-C, C-S and S-S defines the support conditions. C and S are the abbreviation of clamped and simple supports, respectively.

## 6. Conclusions

In this paper, geometric and material nonlinear analyses of gable frame were implemented to achieve the buckling and post-buckling behavior of these frames under static point load. For discretization of members, a high performance element entitled nonlinear beam-column element, which had been formulated based on the displacement-based beam element, was employed in OpenSees software. The cross-section of members was assumed to be I-shape. Different types of support conditions including clamped-clamped, clamped-simple and simple-simple were considered to investigate the effects of boundary conditions on the buckling load. Furthermore, corotational nonlinear principles were utilized due to incorporate large deflections. In addition, a displacement control method (herein arc-length) was also employed to solve the nonlinear equations incrementally. On the other hand, the material nonlinearity was also considered in analyses using Giuffre-Menegotto-Pinto steel material properties based on isotropic hardening. Furthermore, large deflection and rotations were also incorporated by using co-rotational formulation as geometric transformation in OpenSees software. Therefore, the frame was analyzed in two stages so that the effects of geometric and material nonlinearities on the equilibrium paths, buckling and post-buckling behaviors were investigated. Finally, a well-known benchmarks was solved to show the correctness and accuracy of the used model. This example was also solved to perform a convergence study for achieving the minimum number of beam-column element that required for discretization. Moreover, some numerical problems were solved and the related equilibrium paths were obtained separately. The buckling loads of gable frame with different support conditions were also reported. According to the obtained result, the following point can be found out:

- By increasing the slope ratio of the frames, the buckling capacity of the frame decreases.
- Although lower values of slope ratio decrease the vertical displacement of the vertex at the end of loading, it decreases the initial buckling capacity of the frame.
- It is obvious that by considering the material nonlinearity in addition to geometric nonlinearity decreases the initial buckling capacity of the frame while it increases the flexibility of the structure.
- It is observed that the geometric nonlinearity is more effective on the nonlinear behavior of the frame with simple supports compared to those with other support conditions.
- It is obvious that the final vertical displacement of the frame vertex for simply supported

frame is more than that of the fixed-simply supported one.

- In general, the both geometric and material nonlinearities are more effective on the frame with simple supports in comparison with frames with other support conditions.
- Decreasing the initial buckling capacity due to consider material nonlinearity for frame with simple supports is more than that of the frame with fixed supports.
- The amount of decreasing the initial buckling capacity of the frame due to consider material nonlinearity is nearly the same for different values of slope ratio.

## 7. Funding

This research did not receive any specific grant from funding agencies in the public, commercial, or not-for-profit sectors.

## 8. Conflict of Interest

The authors declare that they have no conflict of interest.

## References

- Abbasnia, R. and A. Kassimali (1995), "Large deformation elastic-plastic analysis of space frames", *J. Construct. Steel Res.*, **35**(3), 275-290. [https://doi.org/10.1016/0143-974X\(95\)00008-J](https://doi.org/10.1016/0143-974X(95)00008-J).
- Atlayan, O. and F. A. Charney (2014), "Hybrid buckling-restrained braced frames", *J. Construct. Steel Res.*, **96**, 95-105. <https://doi.org/10.1016/j.jcsr.2014.01.001>.
- Batoz, J.L. and G. Dhatt (1979), "Incremental displacement algorithms for nonlinear problems", *J. Numeric. Method. Eng.*, **14**(8), 1262-1267. <https://doi.org/10.1002/nme.1620140811>.
- Care, R. F., R. E. Lawther and A. P. Kabaila (1977), "Finite element post-buckling analysis for frames", *J. Numeric. Method. Eng.*, **11**(5), 833-849. <https://doi.org/10.1002/nme.1620110506>.
- Chan, S. L. and G. W. M. Ho (1994), "Nonlinear Vibration Analysis of Steel Frames with Semirigid Connections", *J. Struct. Eng.*, **120**(4), 1075-1087. [https://doi.org/10.1061/\(ASCE\)0733-9445\(1994\)120:4\(1075\)](https://doi.org/10.1061/(ASCE)0733-9445(1994)120:4(1075)).
- Chen, H. H., W. Y. Lin and K. M. Hsiao (2006), "Co-rotational finite element formulation for thin-walled beams with generic open section", *Comput. Methods Appl. Mech. Eng.*, **195**(19), 2334-2370. <https://doi.org/10.1016/j.cma.2005.05.011>.
- Clarke, M. J. and G. J. Hancock (1990), "A study of incremental-iterative strategies for non-linear analyses", *J. Numeric. Method. Eng.*, **29**(7), 1365-1391. <https://doi.org/10.1002/nme.1620290702>.
- Crisfield, M. A. (1983), "An arc-length method including line searches and accelerations", *J. Numeric. Method. Eng.*, **19**(9), 1269-1289. <https://doi.org/10.1002/nme.1620190902>.
- Dere, Y. and F. Dede (2011), "Nonlinear finite element analysis of an R/C frame under lateral loading", *Math. Comput. Appl.*, **16**(4), 947. <https://doi.org/10.3390/mca16040947>.
- El-Zanaty, M. H. and D. W. Murray (1983), "Nonlinear finite element analysis of steel frames", *J. Struct. Eng.*, **109**(2), 353-368. [https://doi.org/10.1061/\(ASCE\)0733-9445\(1983\)109:2\(353\)](https://doi.org/10.1061/(ASCE)0733-9445(1983)109:2(353)).
- Fafard, M. and B. Massicotte (1993), "Geometrical interpretation of the arc-length method", *Comput. Struct.*, **46**(4), 603-615. [https://doi.org/10.1016/0045-7949\(93\)90389-U](https://doi.org/10.1016/0045-7949(93)90389-U).
- Filippou, F. C., V. V. Bertero and E. P. Popov (1983), "Effects of bond deterioration on hysteretic behavior of reinforced concrete joints", NSF/CEE-83032, Earthquake Engineering Research Center, University of California, Richmond, CA, USA.

- Fu, Z., K. Ohi, K. Takanashi and X. Lin (1998), "Seismic Behavior of Steel Frames with Semi-Rigid Connections and Braces", *J. Construct. Steel Res.*, **46**(1-3), 440-441.
- Giuffrè, A. (1970), "Il comportamento del cemento armato per sollecitazioni cicliche di forte intensità", *Giornale del Genio Civile*, Istituto di Tecnica Delle Costruzioni, Facolta Di Architettura, Universita Degli Studi di Roma, Italy.
- Goldberg, J. E. and R. M. Richard (1963), "Analysis of non linear structures", *J. Struct. Divison*, **89**(4), 333-351. <https://cedb.asce.org/CEDBsearch/record.jsp?dockkey=0013166>.
- Haisler, W. E., J. A. Stricklin and J. E. Key (1977), "Displacement incrementation in non-linear structural analysis by the self-correcting method", *J. Numeric. Method. Eng.*, **11**(1), 3-10. <https://doi.org/10.1002/nme.1620110103>.
- Hsiao, K. M., J. Y. Lin and W. Y. Lin (1999), "A consistent co-rotational finite element formulation for geometrically nonlinear dynamic analysis of 3-D beams", *Comput. Methods Appl. Mech. Eng.*, **169**(1), 1-18. [https://doi.org/10.1016/S0045-7825\(98\)00152-2](https://doi.org/10.1016/S0045-7825(98)00152-2).
- Jeon, H.M., Y. Lee, P.S. Lee and K.J. Bathe (2015), "The MITC3+ shell element in geometric nonlinear analysis", *Comput. Struct.*, **146**, 91-104. <https://doi.org/10.1016/j.compstruc.2014.09.004>.
- Kassimali, A. and J. J. Garcilazo (2010), "Geometrically nonlinear analysis of plane frames subjected to temperature changes", *J. Struct. Eng.*, **136**(11), 1342-1349. [https://doi.org/10.1061/\(ASCE\)ST.1943-541X.0000233](https://doi.org/10.1061/(ASCE)ST.1943-541X.0000233).
- Liang, K., M. Ruess and M. Abdalla (2016), "Co-rotational finite element formulation used in the Koiter-Newton method for nonlinear buckling analyses", *Finite Element Anal. Design* **116**, 38-54. <https://doi.org/10.1016/j.finel.2016.03.006>.
- Masoodi, A. R. (2018), "Analytical solution for optimum location of belt truss in outrigger system based on stability analysis", *Proceedings of the Institution of Civil Engineers-Structures and Buildings*, **172**(5), 382-388. <https://doi.org/10.1680/jstbu.17.00187>.
- Masoodi, A. R. and S. Heyrani-Moghaddam (2015), "Nonlinear dynamic analysis and natural frequencies of gabled frame having flexible restraints and connections", *KSCE J. Civil Eng.*, **19**(6), 1819-1824. <https://doi.org/10.1007/s12205-015-0285-4>.
- McKenna, F., G. Fenves and M. Scott (2006), "OpenSees: Open system for earthquake engineering simulation", Pacific Earthquake Engineering Research Center, University of California, Berkeley, CA., <http://opensees.berkeley.edu>.
- Memon, B.-A. (2004), "Arc-length technique for nonlinear finite element analysis", *J. Zhejiang U Sci.*, **5**(5), 618-628. <https://doi.org/10.1631/jzus.2004.0618>.
- Menegotto, M. and P. Pinto (1973), "Method of analysis for cyclically loaded reinforced concrete plane frames including changes in geometry and non-elastic behavior of elements under combined normal force and bending", *Proceedings of IABSE Symposium on Resistance and Ultimate Deformability of Structures Acted on by Well-Defined Repeated Loads*, Lisboa, Portugal.
- OpenSees (2006), University of California, Berkeley, USA.
- Oran, C. and A. Kassimali (1976), "Large deformations of framed structures under static and dynamic loads", *Comput. Struct.*, **6**(6), 539-547. [https://doi.org/10.1016/0045-7949\(76\)90050-X](https://doi.org/10.1016/0045-7949(76)90050-X).
- Ottaviani, M. (1975), "Three-dimensional finite element analysis of vertically loaded pile groups", *Géotechnique*, **25**(2), 159-174. <https://doi.org/10.1680/geot.1975.25.2.159>.
- Paullo Muoz, L. F., P. B. Goncalves, R. A. M. Silveira and A. Silva (2017), "Nonlinear resonance analysis of slender portal frames under base excitation", *Shock Vib.*, **2017**, 21. <https://doi.org/10.1155/2017/5281237>.
- Powell, G. and J. Simons (1981), "Improved iteration strategy for nonlinear structures", *J. Numeric. Method. Eng.*, **17**(10), 1455-1467. <https://doi.org/10.1002/nme.1620171003>.
- Rezaiee-Pajand, M., E. Arabi and A. R. Masoodi (2018), "A triangular shell element for geometrically nonlinear analysis", *Acta Mechanica*, **229**(1), 323-342. <https://doi.org/10.1007/s00707-017-1971-8>.
- Rezaiee-Pajand, M. and A. R. Masoodi (2018), "Exact natural frequencies and buckling load of functionally graded material tapered beam-columns considering semi-rigid connections", *J. Vib. Control.*, **24**(9), 1787-1808. <https://doi.org/10.1177/1077546316668932>.
- Rezaiee-Pajand, M. and A. R. Masoodi (2019), "Stability analysis of frame having FG tapered beam-

- column", *J. Steel Struct.*, **19**(2), 446-468. <https://doi.org/10.1007/s13296-018-0133-8>.
- Rezaiee-Pajand, M., A. R. Masoodi and M. Bambaeechee (2018), "Tapered beam-column analysis by analytical solution", *Proceedings of the Institution of Civil Engineers-Structures and Buildings*, 1-16. <https://doi.org/10.1680/jstbu.18.00062>.
- Rezaiee-Pajand, M., A. R. Masoodi and M. Mokhtari (2018), "Static analysis of functionally graded non-prismatic sandwich beams", *Adv. Comput. Design.*, **3**(2), 165-190. <https://doi.org/10.12989/acd.2018.3.2.165>.
- Rezaiee-Pajand, M., M. Mokhtari and A. R. Masoodi (2018), "Stability and free vibration analysis of tapered sandwich columns with functionally graded core and flexible connections", *CEAS Aeronautical J.*, **9**(4), 629-648. <https://doi.org/10.1007/s13272-018-0311-6>.
- Rezaiee-Pajand, M., N. Rajabzadeh-Safaei and A. R. Masoodi (2019), "An efficient mixed interpolated curved element for geometrically nonlinear analysis", *Appl. Math. Modell.*, **76**, 252-273. <https://doi.org/10.1016/j.apm.2019.06.007>.
- Rezaiee-Pajand, M., N. Rajabzadeh-Safaei and A. R. Masoodi (2019), "Linear and geometrically nonlinear analysis of plane structures by using a new locking free triangular element", *Eng. Struct.*, **196**, 1-19. <https://doi.org/10.1016/j.engstruct.2019.109312>.
- Rezaiee Pajand, M., A. Masoodi and A. Alepeighambar Moghadam (2018), "Lateral-torsional buckling of functionally graded tapered I-beams considering lateral bracing", *Steel Compos. Struct.*, **28**(4), 403-414. <https://doi.org/10.12989/scs.2018.28.4.403>.
- Rodrigues, F. C., A. C. Saldanha and M. S. Pfei (1998), "Non-linear Analysis of Steel Plane Frames with Semirigid Connections", *J. Construct. Steel Res.*, **46**, 94-97.
- Rose, G., D. Nguyen and B. Newman (2016), "Implementing an arc-length method for a robust approach in solving systems of nonlinear equations", *IEEE South East Conference*, Norfolk, VA, USA. July. <https://doi.org/10.1109/SECON.2016.7506753>.
- Salawdeh, S. and J. Goggins (2013), "Numerical simulation for steel brace members incorporating a fatigue model", *Eng. Struct.*, **46**, 332-349. <https://doi.org/10.1016/j.engstruct.2012.07.036>.
- Shi, G. and S. N. Atluri (1989), "Static and Dynamic Analysis of Space Frames with Nonlinear Flexible Connections", *J. Numeric. Method. Eng.*, **28**, 2635-2650. <https://doi.org/10.1002/nme.1620281110>.
- Shooshtari, A., S. Heyrani-Moghaddam and A. R. Masoodi (2015), "Pushover analysis of gabled frames with semi-rigid connections", *Steel Compos. Struct.*, **18**(6), 1557-1568. <https://doi.org/10.12989/scs.2015.18.6.1557>.
- Shooshtari, A., A. Masoodi and S. H. Moghaddam (2014), "Free vibration analysis of gabled frame considering elastic supports and semi-rigid connections", *J. Civil, Environ. Struct. Construct. Architect. Eng.*, **8**(6), 701-705.
- Taeprasartsit, S. (2013), "Nonlinear free vibration of thin functionally graded beams using the finite element method", *J. Vib. Control.*, **21**(1), 29-46. <https://doi.org/10.1177/1077546313484506>.
- Thombare, C. N., K. K. Sangle and V. M. Mohitkar (2016), "Nonlinear buckling analysis of 2-D cold-formed steel simple cross-aisle storage rack frames", *J. Build. Eng.*, **7**, 12-22. <https://doi.org/10.1016/j.jobe.2016.05.004>.
- Urthaler, Y. and J. N. Reddy (2005), "A corotational finite element formulation for the analysis of planar beams", *Communications Numeric. Methods Eng.*, **21**(10), 553-570. <https://doi.org/10.1002/cnm.773>.
- Wood, R. D. and O. C. Zienkiewicz (1977), "Geometrically nonlinear finite element analysis of beams, frames, arches and axisymmetric shells", *Comput. Struct.*, **7**(6), 725-735. [https://doi.org/10.1016/0045-7949\(77\)90027-X](https://doi.org/10.1016/0045-7949(77)90027-X).